THE JOURNAL OF COMPARATIVE NEUROLOGY 356:418–432 (1995)

Postsynaptic Gephyrin Immunoreactivity Exhibits a Nearly One-to-One Correspondence With Gamma-Aminobutyric Acid-Like Immunogold-Labeled Synaptic Inputs to Sympathetic Preganglionic Neurons

J.B. CABOT, A. BUSHNELL, V. ALESSI, AND N.R. MENDELL
Department of Neurobiology and Behavior, State University of New York at Stony Brook, Stony Brook, New York 11794-5230

ABSTRACT

Peripheral regulation of cardiovascular function is fundamentally influenced by central excitation and inhibition of sympathetic preganglionic neurons in thoracic spinal cord. This electron microscopy study investigated whether the γ-aminobutyric acid (GABA)-ergic and glycinergic inhibitory innervation of sympathetic preganglionic neurons arises from mutually exclusive afferent populations. Sympathetic preganglionic neurons were retrogradely labeled with cholera β subunit. GABAergic terminals were identified using strict quantitative statistical analyses as those boutons containing significantly elevated levels of GABA-like immunogold labeling ($GABA^+$). Glycinergic terminals were classified as those boutons opposite postsynaptic gephyrin immunostaining containing background levels of GABA-like immunogold labeling ($gephyrin^+/GABA^-$ association). Approximately 43% of the synaptic terminals that contacted sympathetic preganglionic somata and proximal dendrites and that were opposite gephyrin were $GABA^-$; the remaining 57% were $GABA^+$. Only two $GABA^+$ boutons (4%) that synapsed on identified sympathetic preganglionic neuron (SPN) processes were not opposite gephyrin immunostaining ($GABA^+/gephyrin^-$ association). $GABA^-/gephyrin^+$ associations were anticipated given prior anatomical, physiological, and pharmacological data. The observed nearly one-to-one correspondence between postsynaptic gephyrin immunoreactivity and $GABA^+$ boutons was unexpected. Prior physiological and pharmacological experiments suggest that the postsynaptic effects of GABAergic inputs to sympathetic preganglionic neurons are mediated by activation of $GABA_A$ receptors. Those data, the present results, and other molecular, biochemical, and anatomical studies of gephyrin in the central nervous system (CNS) are consistent with two hypotheses: 1) Postsynaptic gephyrin is associated with $GABA_A$ receptors in the membranes of sympathetic preganglionic neurons, and 2) $GABA^+/gephyrin^+$ associations do not necessarily predict colocalization of GABA and glycine within single boutons synapsing on sympathetic preganglionic somata and dendrites.

Indexing terms: autonomic nervous system, glycine receptor, intermediolateral cell column, spinal cord, sympathetic nervous system

Physiological and pharmacological observations suggest that sympathetic preganglionic neurons (SPNs) in mammalian thoracic spinal cord are postsynaptic to afferent inputs that release two different inhibitory amino acid neurotransmitters: γ-aminobutyric acid (GABA) and glycine. Both of these amino acid neurotransmitters have been implicated in the generation of fast inhibitory postsynaptic potentials (fast IPSPs) in SPNs via activation of postsynaptic receptors that open chloride ion channels. SPN membrane hyperpolarization following either synaptic release or exogenous application of GABA is antagonized by the specific

Accepted November 8, 1994.

Address reprint requests to John B. Cabot, PhD, Department of Neurobiology and Behavior, Life Sciences Building, State University of New York at Stony Brook, Stony Brook, NY 11794-5230.

$GABA_A$ receptor antagonist bicuculline (Clendening and Hume, 1990a; Inokuchi et al., 1992). SPN membrane hyperpolarization following either synaptic release or exogenous application of glycine is most often, but not always, abolished by the specific glycine receptor antagonist strychnine (Dun and Mo, 1989; Clendening and Hume, 1990a; Inokuchi et al., 1992).

These physiological and pharmacological data are supported by anatomical observations. GABA-like and glycine-like immunoreactivity has been localized separately within synaptic terminals contacting, or closely apposed to, identified SPN perikarya and dendrites (Bacon and Smith, 1988; Bogan et al., 1989; Cabot et al., 1992; Llewellyn-Smith et al., 1992). In general, putative GABAergic and glycinergic afferent inputs to SPNs are indistinguishable morphologically from one another: Their terminal boutons typically contain mixtures of pleomorphic and round vesicles and form symmetric specializations with postsynaptic SPN processes.

Until recently, there was little reason to suspect that GABAergic and glycinergic afferents to SPNs were anything other than separate populations of terminals arising from different cells of origin (see, e.g., Bogan et al., 1989; Dun and Mo, 1989; Cabot et al., 1992). However, new physiological data indirectly challenge this assumption. Specifically, in slice preparations of cat thoracic spinal cord, Inokuchi et al. (1992) showed that intracellularly recorded fast IPSPs in SPNs were 1) reversibly antagonized by the $GABA_A$ receptor antagonist bicuculline in 32% of SPNs, 2) reversibly antagonized by the glycine receptor antagonist strychnine in 47% of SPNs, and 3) reversibly antagonized by the combination of bicuculline and strychnine in 21% of SPNs. One of several possible interpretations of this last observation is that some axon terminals synapsing on SPNs corelease GABA and glycine. Two electron microscopic studies provide indirect evidence to support this interpretation (Chiba and Semba, 1991; Llewellyn-Smith et al., 1992). 1) The observations of Chiba and Semba (1991) showed that 39% of presumptive GABAergic terminals on unidentified neuronal processes in the SPN neuropil of rats were opposite postsynaptic gephyrin, the 93 kDa protein that is associated with the ligand-binding, membrane-spanning subunits of the glycine receptor (Schmitt et al., 1987; Kirsch et al., 1991, 1993b; Prior et al., 1992; Kirsch and Betz, 1993). 2) The quantitative data reported by Llewellyn-Smith et al. (1992) on glutamatergic and GABAergic inputs to identified SPN processes in the rat SPN neuropil imply that presynaptic release of glycine neurotransmitter could arise from terminals capable of releasing GABA neurotransmitter.

Taking a strictly quantitative approach, the present electron microscopic study was undertaken to reexamine the hypothesis that putative neurotransmitter levels of GABA and glycine are contained in separate populations of afferent terminations on identified SPN processes. GABAergic terminals were identified using postembedding immunogold labeling methods; these data were analyzed using a conservative statistical approach that gives a reliable estimate of the variance of immunogold labeling within synaptic terminals. Glycinergic terminals were identified as those opposite postsynaptic gephyrin immunostaining. The decision to use gephyrin as a marker of glycinergic inputs was predicated on prior observations showing that this 93 kDa peripheral membrane protein is 1) almost exclusively located opposite synaptic boutons (Triller et al., 1985, 1987; Altschuler et al., 1986; Seitanidou et al., 1988; van den Pol and Gorcs, 1988; Wenthold et al., 1988; Smiley and Yazulla, 1990; Chiba and Semba, 1991; Pourcho and Owczarzak, 1991; Yazulla and Studholme, 1991; Zucker and Ehinger, 1992; Chen and Hillman, 1993; Grunert and Wassle, 1993; Mitchell et al., 1993; Sassoè-Pognetto et al., 1994) and 2) associated with both strychnine-sensitive and strychnine-insensitive isoforms of the membrane-spanning subunits of the inhibitory glycine receptor (Pfeiffer et al., 1982; Graham et al., 1985; Schmitt et al., 1987; Becker et al., 1988, 1989; Hoch et al., 1989; Langosch et al., 1990; Sassoè-Pognetto et al., 1994).

The following results show that determining anatomically whether or not GABAergic inputs are distinct from glycinergic inputs depends critically on the underlying assumption that gephyrin colocalizes exclusively with the ligand-binding, membrane-spanning subunits of the glycine receptor. Our observations suggest that this may not be the case and are in agreement with a recent hypothesis that gephyrin can also be commonly associated with postsynaptic regions opposite terminal boutons that may not be releasing glycine (Froehner, 1993; Kirsch and Betz, 1993; Kirsch et al., 1993a). A preliminary account of the results of this work has been published previously in abstract form (Cabot et al., 1993).

MATERIALS AND METHODS

Experimental animals

Experiments were performed on 11 male Sprague Dawley rats, 2–4 months of age, weighing 125–150 g. Rats were obtained from Taconic Farms (Germantown, NY).

Surgical and injection procedures

All surgical procedures were performed under aseptic conditions. Following a subcutaneous injection of atropine (0.3 mg/kg), anesthesia was induced with a subcutaneous injection of a 1:1.8 mixture of rompun (10 mg/kg):ketamine (90 mg/kg). The right superior cervical ganglion (SCG) was approached ventrolaterally following a midline, anterior cutaneous incision extending from approximately the second to the sixth cervical vertebrae.

In all experiments, 1–2 μl of 1% cholera β subunit (CTβ; List Biologicals) was pressure injected into the right SCG through a 10 μl Hamilton syringe to which was affixed a glass micropipette tip (25–50 μm in diameter). Survival time varied from 4 to 5 days.

At the time of sacrifice, rats were given a lethal dose of Nembutal (100 mg/kg). When rats were completely unresponsive to nociceptive stimuli, they were perfused transcardially with 100–200 ml of saline containing 0.1% lidocaine followed by 1 liter of an ice-cold mixture of 4% paraformaldehyde and 0.25–0.5% glutaraldehyde in 0.1 M phosphate buffer (PB, pH 7.4). Spinal cord segments C8 through T3 were removed and postfixed either for 1–2 hours in the perfusion mixture described above or overnight in sodium bicarbonate buffered (0.1 M, pH 9.8) 4% paraformaldehyde.

Preembedding immunohistochemical procedures

Spinal cord segments C8 through T3 were sectioned on a Vibratome at 50 μm in the horizontal plane. Serial order was maintained. The freshly cut sections were examined wet under a light microscope, and the four or five sections

per spinal cord segment most likely to contain SPNs were selected for further processing.

The selected sections were treated for 30 minutes in 1% sodium borohydride (0.1 M PB) and passed through a series of ice-cold, 0.1 M phosphate-buffered alcohols (10%-25%-40%-25%-10%). Following three 10 minute rinses in PB, the sections were placed into 2% normal goat serum (NGS; PB) for 1 hour at room temperature and then transferred into anti-gephyrin (originally called anti-glycine receptor, mAb7a; Boehringer Mannheim, Germany) for 30 minutes at room temperature (1:25–50, 0.3% Triton X-100, PB). Sections were rinsed for 3 × 10 minutes in PB and incubated a second time in antigephyrin for 48–72 hours at 4°C (1:25–50, 2% NGS, 0.004% sodium azide, PB). After a 1 hour rinse in PB, tissue was incubated in biotinylated horse anti-mouse IgG (1:200, PB) for 2 hours at room temperature and was then rinsed 3 × 10 minutes (PB). Sections were then placed into ABC reagent (Vectastain) for 2 hours, rinsed in PB (3 × 10 minutes) and 3 × 10 minutes in acetate buffer (0.1 M, pH 6.0), and reacted for 3 minutes in an acetate-buffered solution containing 0.05% 3,3′-diaminobenzidine HCl (DAB), 0.6% nickel ammonium sulfate, and 0.01% H_2O_2. The tissue was washed 3 × 5 minutes in acetate buffer and 3 × 5 minutes in PB, osmicated (2% OsO_4 for 1 hour), rinsed 3 × 10 minutes in PB, dehydrated through an ascending series of ethanols, and embedded in Epon (Tousimis Research Corp) or Durcupan (Polysciences) between sheets of ACLAR (Allied Chemicals).

Identification of retrogradely labeled SPN processes

Preliminary experiments indicated that immunoperoxidase staining for both CTβ and gephyrin prior to plastic embedding seriously compromised our ability to localize unequivocally postsynaptic gephyrin immunoperoxidase staining in retrogradely labeled processes. Consequently, the following experimental protocol for the identification of retrogradely labeled SPN processes was implemented: 1) Plastic wafers containing gephyrin immunostaining were examined with a Leitz Orthoplan microscope, and regions most likely to contain SPNs were identified. 2) These identified regions were cut out and mounted on blank resin studs, trimmed, and sectioned according to a format in which one "thick" section (~1 μm) was taken and placed on a glass slide for every 10 thin sections (~90 nm) mounted on formvar-coated, single-slot, nickel grids. 3) The 1-μm-thick sections were immunostained for CTβ as described below. 4) Digital images of areas within the 1-μm-thick sections that contained CTβ-labeled SPN somata and dendrites were captured with a DAGE MTI CCD-72S camera system mounted on a Leitz Orthoplan microscope (×20 and ×40 objective magnifications were routinely used; ×100 was used infrequently); the digital images were processed using BioScan Optimas image-analysis software (BioScan, Inc.). 5) The processed images were displayed on a Sony monitor mounted on the front panel of a Jeol 1200EX electron microscope and served as reference guides for the identification of retrogradely labeled SPN somata and dendrites in thin sections adjacent to the image processed "thick" sections (Figs. 1a, 2a). This protocol allowed us to identify 17 SPN somata and 5 SPN dendrites for subsequent analyses. The lower limit on the size of a dendritic process that could be identified using this methodology was approximately 1 μm diameter. Among five SPN dendrites analyzed, two were >4 μm in diameter, two were >2 μm in diameter, and one was ~1 μm in diameter (Fig. 3).

Postembedding immunohistochemical procedures

Immunoperoxidase labeling of CTβ antigen. The protocol used for immunoperoxidase staining of 1-μm-thick plastic sections is a slight modification of protocols used previously (Bogan et al., 1989; Cabot et al., 1992). Sections were cut on a Reichert Ultracut E ultratome, placed on drops of distilled water on gelatin-coated slides, and dried for 30–60 minutes on a hot plate set at 50°C. Slides were placed in a saturated solution of sodium ethanolate for 15 minutes, rinsed 3 × 5 minutes in 100% ethanol and 2 × 5 minutes in distilled water, incubated in 1% sodium periodate for 7 minutes, and washed 2 × 5 minutes in distilled water and 2 × 5 minutes in PB. Sections on the slides were covered with 20% bovine serum albumin (BSA; PB, 0.3% Triton X-100) for 20 minutes, rinsed in PB for 20 minutes, and then incubated in a humidified chamber for 24 hours at 4°C in anti-choleragenoid (List Biologicals) diluted 1:2,000 (PB, 0.3% Triton X-100). Sections were rinsed 3 × 15 minutes in PB, covered with 20% BSA for 30 minutes, and then incubated for 1 hour in biotinylated rabbit anti-goat IgG (1:200, PB, 0.3% Triton X-100). Sections were washed 3 × 10 minutes in PB, placed into ABC reagent (Vectastain, PB, 0.3% Triton X-100) for 1 hour, and rinsed in PB (3 × 10 minutes) and 3 × 10 minutes in acetate buffer (0.1 M, pH 6.0). Sections were then incubated for 3 minutes in an acetate-buffered solution containing 0.05% DAB, 0.6% nickel ammonium sulfate, and 0.01% H_2O_2. The sections were rinsed 3 × 5 minutes in acetate buffer and 3 × 5 minutes in PB, dehydrated through an ascending series of ethanols followed by two changes in xylenes, and coverslipped with Permount. Tissue was examined and photographed on a Leitz Orthoplan microscope equipped with Nomarski contrast interference optics and/or was digitally imaged as described above.

Immunogold labeling of GABA-like antigen for electron microscopy. The methods were those used previously by our group (Cabot et al., 1992) and are a modification of the droplet, on-grid procedures of Somogyi and Soltesz (1986). After etching and deosmication, the specific steps implemented and the reagents used were those recommended by the supplier of the gold-labeled goat anti-rabbit Igs (Auro-Probe EM GAR G15; Amersham International). Incubations in anti-GABA (Sigma Immunochemicals) primary antiserum were overnight (18–20 hours) at room temperature at a dilution of 1:750. Incubations in gold-labeled goat anti-rabbit Igs were for 4 hours at a dilution of 1:25. After extensive rinsing, grids were placed in 2% glutaraldehyde (PB) for 10 minutes, rinsed 3 × 5 minutes in PB and 2 × 5 minutes in distilled H_2O, and stained with uranyl acetate and lead citrate. Grids were examined and photographed on Jeol 1200EX electron microscope.

Immunogold data analysis

The statistical "cutoff" criteria for distinguishing GABA-like immunogold-labeled synaptic terminals (i.e., $GABA^+$ terminals) from background (i.e., $GABA^-$ terminals) were derived from analyses of >48,000 μm^2 of tissue sampled from the neuropil surrounding SPNs in the intermediolateral cell column (IML) and nucleus intercalatus (IC) in spinal cord segments T1–T2. Six separate and independent

statistical analyses were performed, and the density of gold particles (number of gold particles/μm^2) was from 17 SPN somata and 1,341 synaptic terminals (Table 1, Figs. 5, 6).

The subjective criteria for initiating the generation of a photomontage for subsequent analysis were similar to those used in prior investigations (Bogan et al., 1989; Cabot et al., 1992). First, a synaptic terminal(s) contacting a retrogradely CTβ-labeled SPN process was identified. Second, this bouton had to appear to have an immunogold labeling density greater than a subjective estimate of the background labeling in the tissue section. Third, the identified terminal had to be immunogold labeled in two or more serial thin sections. These three criteria are neither necessary nor sufficient conditions for performing the statistical analysis described below, but they were implemented routinely, because our goal was to identify $GABA^+$ synaptic inputs to SPN processes.

Upon satisfaction of the subjective criteria, a nonoverlapping photomontage containing >50 synaptic terminals was obtained. The approximate center of the montage included the terminal(s) subjectively identified as containing elevated immunogold labeling. If necessary, additional electron micrographs of CTβ-labeled SPN perikarya were acquired from contiguous or noncontiguous regions on the same thin section if significant proportions of two or more SPN perikarya were not included in the initial montage (with a single exception, in which this was not possible; see case 2919IC in Table 1). The density of gold particles (number of gold particles/μm^2) was tabulated for both terminals and SPN perikarya; gold particles overlying mitochondria were excluded from all measurements.

In SPN perikarya, two procedures were implemented (see justification immediately below). In the first, the number of gold particles/total somal area was measured. In the second, immunogold densities in SPN perikarya were sampled with a synaptic terminal-sized template (TSA; terminal sample area). The TSA chosen for a particular analysis was the actual outline of a terminal included in the sample; the area of this terminal was approximately equal to the average synaptic terminal area calculated from the entire sample being analyzed (Table 1). The minimum number of TSA samples/SPN soma was 27; the maximum was 108. The total number of TSA sample areas/analysis ranged from 54 (case 2789T) to 200 (cases 2838D and 2938QC). In the analysis in which only a single SPN (case 2919IC) was in the thin section analyzed, data were acquired on 108 TSAs. Nuclear areas were excluded from sampling.

To ascertain statistically whether a synaptic bouton was $GABA^+$, an estimate of "background" (specific + nonspecific) labeling had to be determined. ("Specific" background labeling might include labeling of an antigen being utilized in a metabolic pathway, whereas "nonspecific" background would include immunogold labeling generated by nonspecific binding of primary or secondary antibodies.) In a prior investigation, it was possible to show that estimates of "background" immunogold labeling (i.e., $GABA^-$ labeling) could be obtained by sampling only synaptic terminals; the "specific" component of "background" appeared to be minimal in the neuropil surrounding SPNs (Bogan et al., 1989). However, a limitation of this analytic approach was that terminals containing zero gold particles were ignored. For the present study, we developed a statistical methodology that removes this bias and that is more generally applicable to analyses of other amino acid neurotransmitter molecules (Cabot et al., 1994).

The cellular elements chosen for estimating background $GABA^-$ immunogold labeling were SPN somata. This choice was predicated on the following general and specific considerations. 1) "Background" immunogold labeling would probably be best estimated in a neuronal element, because comparisons to a second neuronal element, synaptic terminals, were to be made. 2) The neuronal element used to estimate "background" immunogold labeling should not be involved in neurotransmitter synthesis of GABA; not to impose this limitation would result in measurements inclusive of the parameter to be distinguished, with no obvious way to factor out the unwanted observations. 3) Prior light and electron microscopic investigations established that SPNs were not GABAergic (Bacon and Smith, 1988; Bogan et al., 1989).

Using neuronal perikarya to estimate "background" immunogold labeling for putative neurotransmitter candidates is not an unusual procedure (see, e.g., Llewellyn-Smith et al., 1992). Typically, such estimates of "background" labeling are determined by measuring mean somal labeling (number of gold particles/total cell body area), followed by taking an average over two or more somata. A standard deviation about the mean somal density is estimated, and, then, a cutoff criterion density value is generated. (For example, mean somal density + 2.58 × standard deviation: This calculation assumes a normal distribution of "background" densities, and the cutoff criterion value corresponds to the upper 99.5th percentile; immunogold labeling densities in synaptic terminals above the criterion cutoff value are presumed to indicate the localization of putative neurotransmitter levels.) The mean of the densities observed is taken as an unbiased estimate of mean somal density; this quantity, in turn, serves as the estimate of mean "background" density in synaptic terminals.

The parameters for "background" were estimated here using the observed densities in SPNs. However, because soma area was much greater than the size of an average synaptic bouton, one could not use the observed standard deviation of the densities across somata as a direct estimate of the standard deviation of a terminal size area within a soma. Instead, the standard deviation of a terminal size area was estimated using variance components analysis of the observed densities of terminal size areas within SPN somata (random effects model; Snedecor and Cochran, 1989). The argument for this is as follows: The density of GABA-like immunogold labeling in an SPN soma can be calculated as

$$\text{Density}_{\text{SOMAL AREA}} = D_{\text{SOMAL AREA}} = \text{No. of gold particles/A}, \quad (1)$$

where A = somal area. Because somal area (A) is much larger than the area of an average-sized synaptic terminal (terminal size area; TSA), $D_{\text{SOMAL AREA}}$ can be expressed as a sample mean of densities in TSAs as follows: Let TSA equal the average terminal sampling area in a given sample; then

$$\text{A/TSA} = \text{r where r} = \text{the number of TSAs per SPN soma.} \quad (2)$$

If we divide a somal area into r such TSAs, then, from Equations 1 and 2,

$$D_{\text{SOMAL AREA}} = \text{No. of gold particles/A} = \text{No. of gold particles/(r} \times \text{TSA)}. \quad (3)$$

We could, instead, let X_i denote number of gold particles in the ith TSA and conclude that

$$D_{\text{SOMAL AREA}} = \text{No. of gold particles}/(r \times \text{TSA}) = \Sigma(X_i)/(r \times \text{TSA}), \text{ for } i = 1, 2 \ldots r. \quad (4)$$

Now, let d_i denote the immunogold density in the ith TSA within a somal area of size r × TSA. Then

$$d_i = X_i/\text{TSA}. \quad (5)$$

The average (m) of these densities would be

$$m = \Sigma (d_i)/r = \Sigma (X_i/\text{TSA})/r = \Sigma (X_i)/(r \times \text{TSA}) = D_{\text{SOMAL AREA}}. \quad (6)$$

Once it is acknowledged that the immunogold density observed in a SPN soma ($D_{\text{SOMAL AREA}}$) can be expressed as an average (m) of densities (d_i) observed in "r" terminal size areas (TSAs), then it is necessary to be aware that the standard deviation of the values across several SPN somata, when total somal area [STD ($D_{\text{SOMAL AREA}}$)] is used, is much less than the standard deviation of observations made with TSAs STD(d). Specifically, if there is no correlation between TSA densities within a given area of a SPN somata, then, for a sample mean,

$$\text{STD}(m) = \text{STD}(d)/\sqrt{r} = \text{STD}(D_{\text{SOMAL AREA}}) = \text{STD}_{\text{SOMAL AREA}}. \quad (7)$$

What we are interested in, however, is the standard deviation of d, the immunogold density observed in terminal size areas. We see from Equations 1–7 that

$$\text{STD}(d) = \text{STD}_{\text{TSA}} = \text{STD}(X/\text{TSA}) = \text{STD}_{\text{SOMAL AREA}} \times \sqrt{r}. \quad (8)$$

Given the above general relationship (Eq. 8), it is clear that the observed $\text{STD}_{\text{SOMAL AREA}}$ can underestimate STD_{TSA} by as much as a factor of $\sqrt{r}$. Because 1) measurements in SPN somata were to be used as estimators of "background" immunogold labeling, 2) significance comparisons were to be made with density measurements within synaptic terminals, and 3) there was the desire to minimize methodologically generated measurement errors, the present study used the estimated standard deviation of terminal size area density measurements [STD(d) or STD_{TSA}] to generate cutoff criteria for each individual sample. This was accomplished by using variance component analysis of the densities observed in TSAs within SPN somata. This allows for correlation between densities within TSAs taken from the same SPN soma. STD(d) (i.e., STD_{TSA}) was estimated as the square root of the estimated variance of d [i.e., VAR(d)] as follows:

$$\text{STD}(d) = \sqrt{[\text{VAR}(d)]} = \sqrt{[\text{VAR}(X/\text{TSA})]} = \text{STD}_{\text{TSA}}. \quad (9)$$

The VAR(d) of a randomly observed density from a randomly chosen SPN soma is the sum of 1) the variance between different SPN somata ($\text{VAR}_{\text{BETWEEN}}$) and 2) the variance between densities within the same SPN soma ($\text{VAR}_{\text{WITHIN}}$). That is,

$$\text{VAR}(d) = \text{VAR}_{\text{BETWEEN}} + \text{VAR}_{\text{WITHIN}}. \quad (10)$$

Let $\text{MS}_{\text{BETWEEN}}$ denote the sample mean squared error between densities observed in SPN somata computed by an analysis of variance of a sample of S (total number of SPNs sampled) from which we take r, TSA measurements per SPN (r = number of d_is sampled/SPN soma). Let $\text{MS}_{\text{WITHIN}}$ denote the sample mean squared error of d_is within SPN somata. Let $\hat{\text{VAR}}_{\text{WITHIN}}$ denote our estimate of $\text{VAR}_{\text{WITHIN}}$ and let $\hat{\text{VAR}}_{\text{BETWEEN}}$ denote our estimate of $\text{VAR}_{\text{BETWEEN}}$. We obtained estimates of VAR(d) in the usual manner for variance component analysis.

$$\hat{\text{VAR}}_{\text{WITHIN}} = \text{MS}_{\text{WITHIN}}, \quad (11)$$

and

$$\hat{\text{VAR}}_{\text{BETWEEN}} = (\text{MS}_{\text{BETWEEN}} - \text{MS}_{\text{WITHIN}})/r. \quad (12)$$

Applying Equation 10, we estimated VAR(d) by $\hat{\text{VAR}}(d)$ as follows:

$$\hat{\text{VAR}}(d) = \hat{\text{VAR}}_{\text{BETWEEN}} + \hat{\text{VAR}}_{\text{WITHIN}} \quad (13)$$

or

$$\hat{\text{VAR}}(d) = \hat{\text{VAR}}_{\text{WITHIN}}, \text{ whenever } \hat{\text{VAR}}_{\text{BETWEEN}} \leq 0. \quad (14)$$

The values of r in our samples of SPN somata ranged from 27 to 50 for values of S (No. of SPN somata sampled) ranging from 2 to 5 (Table 1). In any given analysis, r was held constant (i.e., we sampled an equal number of TSAs/SPN).

Cutoff criterion immunogold density values (Table 1) for individual samples were determined as follows: A mean somal immunogold density value was calculated as

$$\text{SOMAL MEAN}_{\text{TSA}} = \Sigma_j [\Sigma_i(d_i)/r]/S, \text{ for } i = 1 \ldots r \text{ for } j = 1 \ldots S. \quad (15)$$

Then,

$$\text{Cutoff Criterion} = \text{SOMAL MEAN}_{\text{TSA}} + (2.58 \times \sqrt{[\hat{\text{VAR}}(d)]}) = \text{SOMAL MEAN}_{\text{TSA}} + (2.58 \times \text{STD}_{\text{TSA}}). \quad (16)$$

This cutoff criterion corresponds to a level of significance with a P value < 0.005. That is, in any given sample, immunogold density values in synaptic terminals greater than the cutoff density value have a probability of $< 0.5\%$ of being observed in SPN somata and have been identified as $GABA^+$.

The last column in Table 1 lists the empirically derived estimates of the magnitudes by which the standard deviation of terminal immunogold sampling would have been underestimated if somal area rather than TSA measurements had been used; in no sample would $\text{STD}_{\text{SOMAL AREA}}$

TABLE 1. Statistics for GABA-Like Immunogold Labeling of SPN Perikarya

Case no.	TSA (μm^2)[1]	Somal $mean_{TSA}$ (gold particles/μm^2)[2]	Standard deviation (STD_{TSA})[3]	Cutoff criterion (gold particles/μm^2)[4]	STD_{TSA}/ $STD_{SOMAL\ AREA}$[5]
2919IC	0.961	2.28 (S = 1)[6]	1.33	5.72	—[7]
2659P	0.823	5.66 (S = 3)	3.13	13.73	2.88
2938QC	1.212	1.69 (S = 5)	1.46	5.46	4.96
2659R	0.892	3.59 (S = 2)	1.94	8.59	19.75
2789T	0.953	3.33 (S = 2)	2.21	9.04	3.89
2838D	0.914	2.85 (S = 4)	2.07	8.20	5.04

[1]TSA, terminal sample area (approximately equal to the mean terminal area in a particular sample).
[2]Somal $mean_{TSA}$ = mean # gold particles/SPN soma with random sampling using TSAs.
[3]STD_{TSA}, estimated standard deviation determined by analysis of variance [equals √(estimated variance between cells + estimated variance within cells)]. See Materials and Methods for further details.
[4]Somal $mean_{TSA}$ + (2.58 × STD_{TSA}) ($P < 0.005$). A bouton was considered $GABA^+$ when the immunogold density within it was greater than the criterion density.
[5]$STD_{SOMAL\ AREA}$, observed standard deviation of the individual SPN somal gold densities.
[6]S, number of SPNs sampled.
[7]Ratio could not be calculated, because only one SPN was in the sampled thin section.

have been a good estimator of the variability of measuring immunogold densities in synaptic terminals.

Antibody specificity

All antibodies were purchased commercially. The monoclonal anti-gephyrin antibody (clone R7A) used in the present experiments is specific for the 93 kDa peripheral membrane protein associated with the inhibitory glycine receptor complex (Pfeiffer et al., 1984; Schmitt et al., 1987). At present there is no known eukaryotic protein that is significantly homologous to gephyrin (Prior et al., 1992). When either the primary or the secondary antibody incubation steps were omitted, anti-gephyrin, anti-GABA, and anti-choleragenoid immunolabeling were eliminated. Furthermore, 1) immunostaining for CTβ antigen was negative in thoracic spinal cord tissue taken from segments (T6–T7) that did not contain retrogradely labeled SPNs and 2) preabsorption of anti-GABA (1:500) with 1 mM and 0.5 mM free GABA (Sigma) eliminated or reduced to background levels immunogold labeling of endogenous GABA antigen.

RESULTS

Localization of gephyrin immunoreactivity

We examined the SPN neuropil in all four subnuclei (Il_p or IML, nucleus intermediolateralis, pars principalis; Il_f, nucleus intermediolateralis, pars funicularis; CA, central autonomic area; IC, nucleus intercalatus) for the distribution and localization of postsynaptic gephyrin immunoreactivity (Figs. 1, 2). An unexpected observation was that retrogradely labeled, as well as unidentified, somata and dendrites in all subnuclei exhibited a relatively high density of postsynaptic gephyrin immunostaining. In fact, the density was considerably greater than had been anticipated given prior data on the localization of glycine-like-immunoreactive synaptic inputs to SPNs specifically and to unidentified processes within the SPN neuropil generally (Cabot et al., 1992).

The localization and appearance of gephyrin immunoperoxidase staining within both SPN and unidentified processes resembled that described in prior electron microscopic investigations of other regions of vertebrate and invertebrate nervous system using preembedding, enzymatic DAB-peroxidase methods. Gephyrin immunoreactivity was easily identified as an electron-dense, nickel-enhanced, DAB-peroxidase reaction product (see, e.g., Fig. 1b). Immunostaining was homogeneously dark in appearance and was restricted to patches of peripheral membrane on the cytoplasmic face (Figs. 1c, 2b, 3, 4, 7). Gephyrin immunoreactivity, in addition to being very closely associated with the cytoplasmic face of dendritic and somatic postsynaptic membranes, also was typically observed to extend away from this region into the immediately adjacent and underlying cytoplasm (Figs. 1b,c, 2b, 3, 4, 7).

Postsynaptic gephyrin immunoreactivity was always opposite a presynaptic bouton. The darkest and most intense immunostaining appeared in peripheral membrane regions that overlapped areas of synaptic specialization (Figs. 1c, 3, 4, 7). Presynaptic terminal membrane thickening was frequently observed when postsynaptic gephyrin immunostaining was present. Also, in several analyses of serial sections, it was found that postsynaptic gephyrin immunoreactivity significantly diminished or disappeared when evidence of a synaptic specialization was absent or equivocal (Fig. 4). The general observations described above were true of material immunostained only for gephyrin as well as in tissue that was double labeled (i.e., immunoperoxidase stained for gephyrin and immunogold labeled for GABA).

Identification of $GABA^+$ terminals in the SPN neuropil

Cutoff criterion values for the statistical identification of $GABA^+$ (i.e., GABA-like) immunogold labeling in synaptic terminals were generated from a total of 641 TSA measurements in 17 SPN somata (Table 1). Six separate and independent statistical analyses were performed. The frequency distributions of immunogold densities within sampled SPN somata and synaptic terminals are plotted in Figure 5.

Fig. 1. (Figure appears on page 424.) Light and electron micrographs of a retrogradely, cholera toxin β (CTβ)-labeled sympathetic preganglionic neuron receiving γ-aminobutyric acid $(GABA)^+$ and GABA synaptic inputs; both types of inputs are associated with postsynaptic gephyrin. **a:** Light photomicrograph of a 1 μm horizontal section through a CTβ-labeled sympathetic preganglionic neuron located in the nucleus intercalatus (IC). The asterisk identifies a blood vessel that is similarly identified in b. **b:** Electron micrograph of the IC neuron shown in a. This thin section is ~0.9 μm removed from the 1 μm section in a. Arrowheads point to several peripheral membrane regions exhibiting postsynaptic gephyrin immunostaining. The boxed area is shown at higher magnification in c. N, nucleus. **c:** Electron micrograph showing postsynaptic gephyrin immunostaining associated with $GABA^+$ (arrow) and $GABA^-$ (arrowhead) synaptic inputs to the soma of a sympathetic preganglionic neuron. Scale bars = 10 μm in a, 5 μm in b, 0.5 μm in c.

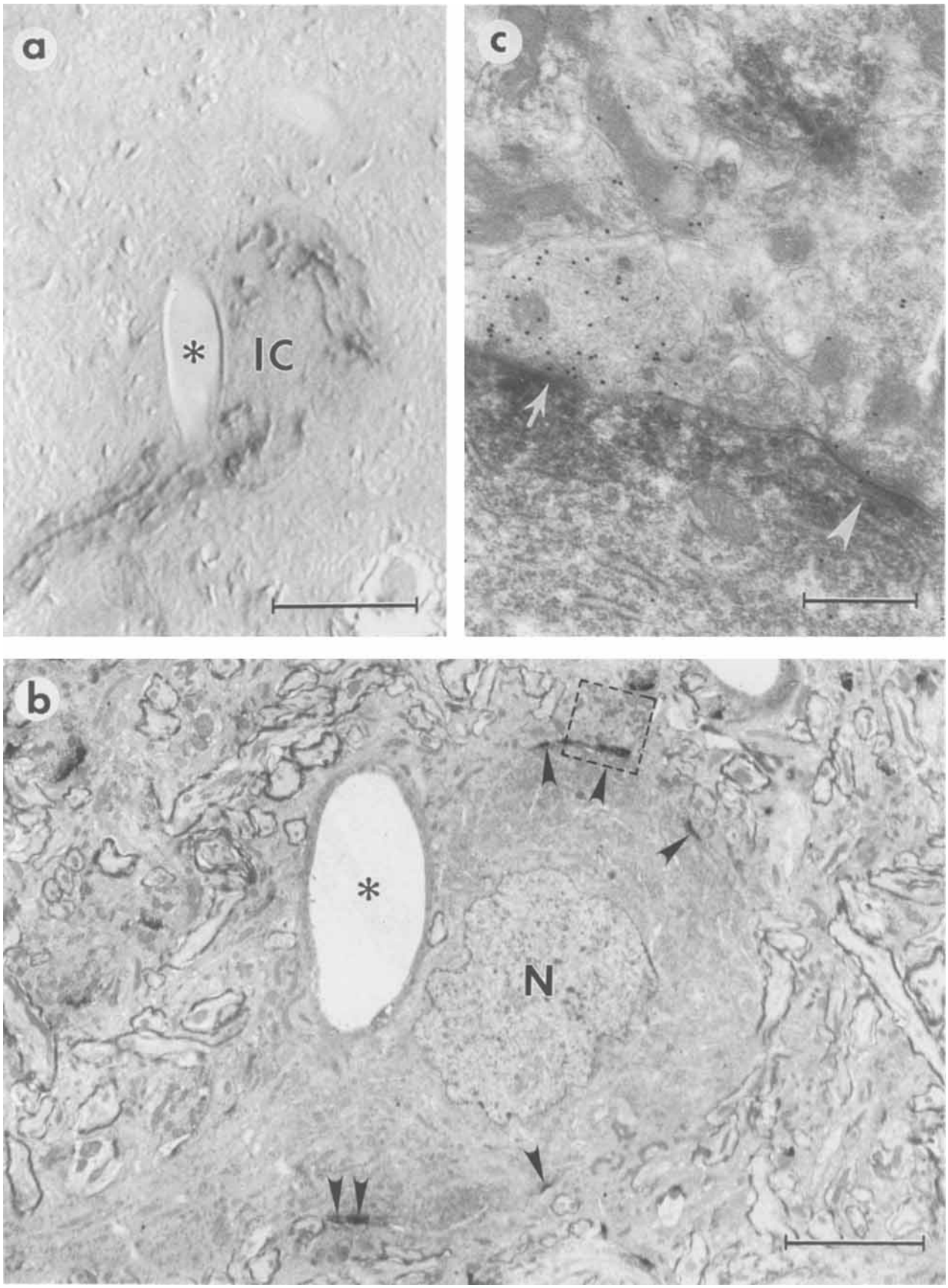

Figure 1

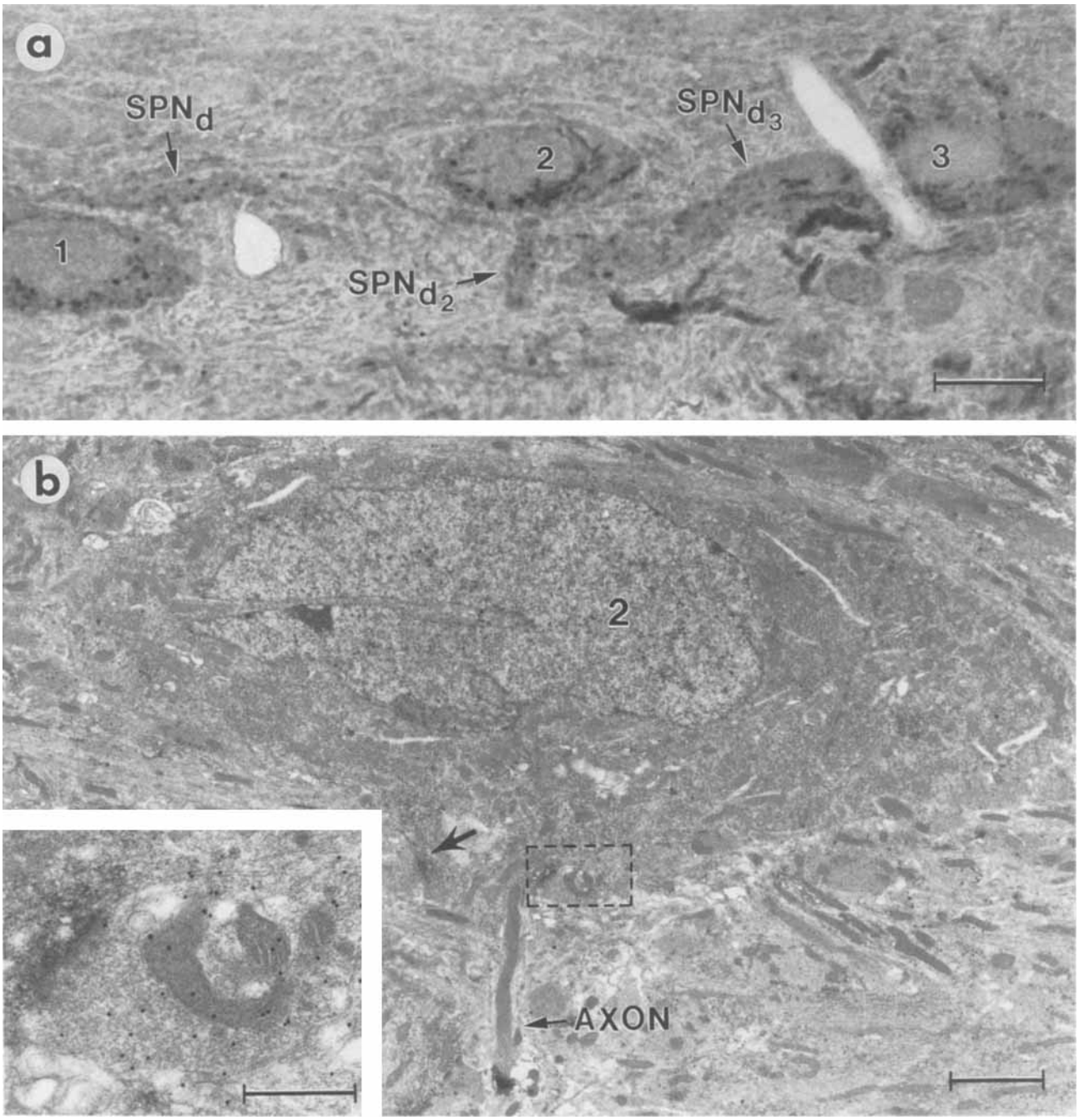

Fig. 2. Light and electron micrographs showing CTβ-labeled sympathetic preganglionic somata and dendrites and an association between postsynaptic gephyrin immunoreactivity and a GABA$^+$ synaptic input to an identified preganglionic soma. **a:** Light photomicrograph of a 1 μm horizontal section through the intermediolateral cell column (IML). Three (1, 2, 3) sympathetic preganglionic somata and three preganglionic dendrites (SPN_d, SPN_{d2}, SPN_{d3}) are identified as being retrogradely labeled with CTβ. **b:** Low-power electron micrograph of the sympathetic preganglionic soma labeled 2 in a. This thin section is immediately adjacent (serial) to the "thick" section in a. The arrow points to postsynaptic gephyrin immunostaining opposite a GABA$^+$ (not shown) synaptic terminal input. The AXON arrow points to the axon of this preganglionic neuron just distal to its site of somal origination. The box outlines a region immediately proximal to the site of axon origination and is shown at higher power in the inset. **Inset:** Electron micrograph showing a GABA$^+$ terminal associated with postsynaptic gephyrin immunoreactivity in the peripheral membrane region immediately proximal to the site of axon origination. Scale bars = 10 μm in a, 2 μm in b, 0.5 μm in inset.

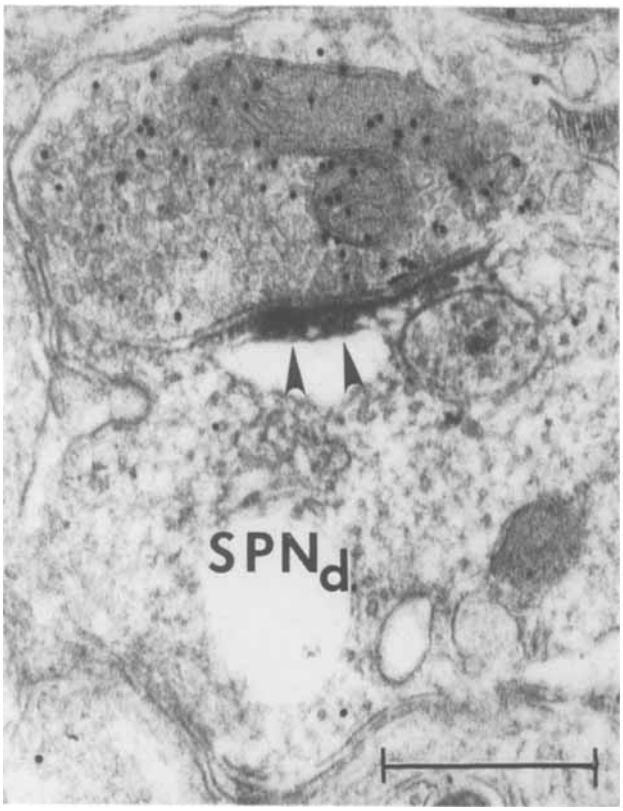

Fig. 3. Electron micrograph showing an immunogold-labeled, GABA$^+$ terminal bouton associated with postsynaptic gephyrin immunostaining (arrowheads) in peripheral membrane of a sympathetic preganglionic dendrite (SPN_d). Scale bar = 0.5 μm.

Gold particle densities (No. of gold particles/μm^2) were calculated for 1,341 boutons (Fig. 6). Among this total, 12.4% (n = 166) of synaptic terminals synapsed with, or were in close apposition to, retrogradely labeled SPN processes. (Close apposition was defined as directly adjacent pre- and postsynaptic membrane regions and the absence of a synaptic specialization.) Approximately 46% of all synaptic terminal associations with identified SPN somata and dendrites were GABA$^+$.

The majority (87.6%) of sampled terminals synapsed with, or were closely apposed to, somata and dendritic elements that were unidentified (Fig. 6). The percentage of GABA$^+$ terminals on unidentified processes (36.2%) in the SPN neuropil generally was less than that observed specifically on identified SPN perikarya and dendrites. On average, 37.4% (n = 502) of all terminals (identified and unidentified) characterized in the SPN neuropil in T1–T2 were GABA$^+$.

Relationships between immunogold terminal labeling for GABA and postsynaptic gephyrin

Retrogradely labeled sympathetic preganglionic processes. In double-labeled tissue, the density of immunogold labeling for GABA was determined for every terminal opposite postsynaptic gephyrin immunoreactivity within a given sample (Fig. 6). Among a total sample of 1,341 synaptic terminals, 166 (12.4%) were closely apposed to, or synapsed with, retrogradely labeled SPN processes. Postsynaptic gephyrin immunoreactivity was directly opposite 50.6% (n = 84) of terminals synapsing on identified SPN somata and dendrites; 57.1% (n = 48) of the terminals associated with postsynaptic gephyrin immunoreactivity were GABA$^+$ (Figs. 1c, 2b, 3, 4). The remaining 42.9% (n = 36) of terminals opposite postsynaptic gephyrin immunoreactivity had immunogold labeling densities that did not differ from background and were classified as GABA$^-$ (Fig. 1c).

Unbiased characterization of the relationship between GABA$^+$ terminal labeling and postsynaptic gephyrin immunoreactivity was achieved by requiring 1) the presence of postsynaptic gephyrin immunoreactivity within the immediately surrounding region being characterized and 2) the unambiguous presence of a synaptic specialization if postsynaptic gephyrin immunostaining was not opposite a GABA$^+$ bouton. The first condition reflects the fact that immunostaining for gephyrin was restricted to the upper 5–10 μm of each block face; thus, visualization of local gephyrin immunostaining was the only unequivocal, internal control for its presence or absence. The second condition acknowledges the fact that gephyrin is restricted to peripheral membrane regions that overlap areas of synaptic contact (see, e.g., Fig. 4). When these conditional requirements were met, all but two GABA$^+$ terminals were found to be opposite postsynaptic gephyrin immunoreactivity (96%, n = 48; Fig. 6). In the two exceptions, the synaptic specialization was symmetric, a configuration typical of the vast majority of GABAergic inputs to SPN processes (Bacon and Smith, 1988; Bogan et al., 1989). Approximately 35% (n = 27) of GABA$^+$ terminals could not be classified, because there was no synaptic specialization present (Fig. 6).

Unidentified processes in the neuropil surrounding sympathetic preganglionic neurons. The ordinal relationships between presynaptic GABA immunogold labeling and postsynaptic gephyrin immunostaining for unidentified processes were essentially similar to those observed for retrogradely labeled SPN processes. Postsynaptic gephyrin immunoreactivity was associated with both GABA$^+$ terminals (43.8%, n = 177) as well as GABA$^-$ terminals (56.2%, n = 227; Figs. 6, 7). Furthermore, when the conditional requirements outlined directly above were met, the overwhelming majority of GABA$^+$ terminals in the SPN neuropil were opposite postsynaptic gephyrin immunoreactivity (95.2%, n = 177; Fig. 6).

DISCUSSION

Methodological considerations

There are two methodological issues that merit discussion, insofar as they significantly influenced our conclusions. First, we introduced a statistical approach for the unbiased analysis of immunogold labeling of synaptic terminals for GABA-like immunoreactivity. The approach is quite conservative and provides an accurate estimate of the variance of immunogold labeling within synaptic terminals. In principle, the method can be applied generally whenever immunogold labeling is employed for the purpose of identifying putative neurotransmitters (see, e.g., Cabot et al., 1994). Importantly, the method provides a surrogate test of one of the fundamental criteria that must be met by any neurotransmitter candidate, namely, that the concentration of a putative neurotransmitter molecule be uniquely elevated in synaptic terminals. In the present experiments, elevated concentrations were likely to be present by virtue of the fact that GABA$^+$ terminals had immunogold densi-

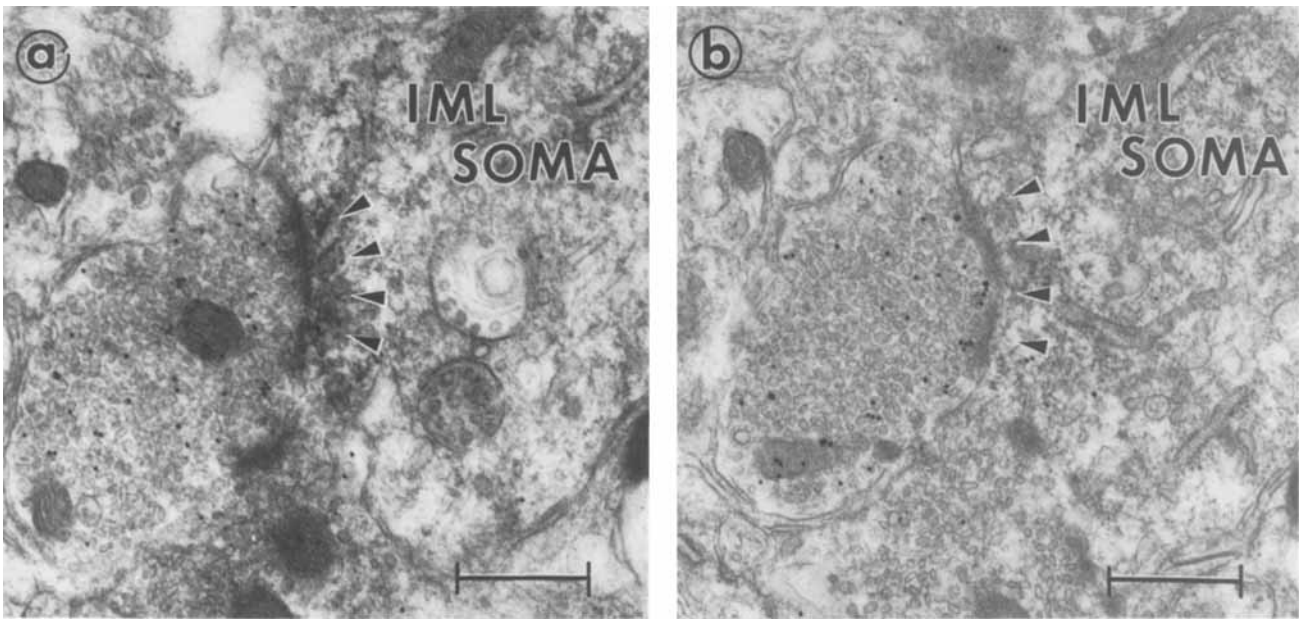

Fig. 4. Electron micrographs showing the localization of postsynaptic gephyrin to a region of synaptic specialization; a and b are serial to one another. The electron micrograph in b is 4 thin sections (~0.36 μm) removed from the electron micrograph in a. **a:** Electron micrograph showing postsynaptic gephyrin immunoreactivity (arrowheads) associated with a GABA$^+$ synaptic terminal contacting the soma of a sympathetic preganglionic neuron in the nucleus intermediolateralis, pars principalis (IML SOMA). **b:** Electron micrograph showing the same terminal in a region removed from the area containing the synaptic specialization. Note the lack of postsynaptic gephyrin immunostaining in the region underlying the arrowheads. Scale bars = 0.5 μm.

ties that would be observed only 0.5% of the time in a non-GABAergic neuronal element. The criterion that a non-GABAergic neuronal element be sampled in order to estimate background labeling is a key initial condition. The non-GABAergic elements used to estimate density distributions of background (i.e., GABA$^-$) immunogold labeling were SPN perikarya. This choice represents a compromise in the present experiments. Our statistical approach would be more robust if the immunogold density distributions of background labeling were estimated by sampling a population of synaptic terminals known, a priori, to be GABA$^-$; such a population of terminals cannot be unequivocally identified in the SPN neuropil at present.

A second methodological issue is the criteria for the classification of an association between a GABA$^+$ terminal and postsynaptic gephyrin immunostaining (i.e., GABA$^+$/gephyrin$^+$ vs. GABA$^+$/gephyrin$^-$ associations). We required that, to conclude that a GABA$^+$ terminal was not opposite postsynaptic gephyrin, there had to be clear evidence of an immunonegative synaptic specialization. Not to impose this conditional exigency would have ignored evidence that gephyrin colocalizes almost exclusively with regions of synaptic contact (Triller et al., 1985, 1987; Altschuler et al., 1986; Seitanidou et al., 1988; van den Pol and Gorcs, 1988; Wenthold et al., 1988; Smiley and Yazulla, 1990; Chiba and Semba, 1991; Pourcho and Owczarzak, 1991; Yazulla and Studholme, 1991; Nicola et al., 1992; Zucker and Ehinger, 1992; Chen and Hillman, 1993; Grunert and Wassle, 1993; Kirsch et al., 1993b; Mitchell et al., 1993; Sassoè-Pognetto et al., 1994). Inclusion of this criterion has led to the outcome that we were unable to replicate a prior observation suggesting that the majority (>60%) of GABAergic boutons in the SPN neuropil of upper thoracic spinal cord are not associated with postsynaptic gephyrin (Chiba and Semba, 1991).

Gephyrin immunostaining and its relationship to GABAergic and non-GABAergic afferent inputs to sympathetic preganglionic neurons

Interpretation of the anatomical results and suggestions about their potential physiological implications depend critically on how one assesses the significance of gephyrin localization. The literature on the identification and characterization of the inhibitory glycine receptor complex argues very convincingly that 1) gephyrin is a peripheral membrane protein that copurifies with the membrane spanning, ligand-binding α and β subunits of the receptor complex (Pfeiffer et al., 1982; Graham et al., 1985; Schmitt et al., 1987; Langosch et al., 1990); 2) gephyrin binds to tubulin and, therefore, may be integrally involved in the anchoring of the subunits of the glycine receptor complex to restricted postsynaptic membrane domains (Kirsch et al., 1991; Prior et al., 1992); 3) gephyrin, in its capacity as a peripheral membrane protein, is not required for the expression of strychnine-sensitive or -insensitive, glycine-gated Cl$^-$ channels in either *Xenopus* oocytes or the mammalian 293 cell line (review by Betz, 1992; see also Schmieden et al., 1989, 1992; Grenningloh et al., 1990; Kuhse et al., 1990a,b, 1993; Akagi et al., 1991a,b; Malosio et al., 1991a,b; Vandenberg et al., 1992a,b; Bormann et al. 1993); 4) gephyrin is necessary for glycine receptor clustering in cell cultures of spinal neurons (Kirsch et al., 1993b).

All the above-mentioned data are consistent with the proposal that GABA$^-$/gephyrin$^+$ associations identify synaptic sites likely to be involved in the presynaptic release of

the neurotransmitter glycine. This conclusion extends and lends further support to prior anatomical and physiological data suggesting that glycine is an inhibitory neurotransmitter input to SPNs (Backman and Henry, 1983; Mo and Dun, 1987; Dun and Mo, 1989; Clendening and Hume, 1990a,b; Cabot et al., 1992; Inokuchi et al., 1992). The observations demonstrating the existence of a distinct population of $GABA^-$/$gephyrin^+$ associations also suggest that there is a glycinergic input to SPNs that is separate from a GABAergic innervation. We did not observe one of the relationships described by Chen and Hillman (1993) as occurring in cerebellum; that is, $GABA^-$ boutons opposite gephyrin immunostaining ($GABA^-$/$gephyrin^+$ association) were not seen forming a second $GABA^+$/$gephyrin^+$ association with the same postsynaptic element. Our observations, however, carry with them a critical caveat: Serial section analyses were only selectively, and not routinely, performed in the present study.

The associations with identified and unidentified neuronal processes in the SPN neuropil between $GABA^+$ synaptic terminals and postsynaptic gephryin immunostaining (i.e., $GABA^+$/$gephyrin^+$ associations) can be interpreted most simply in either of two ways: 1) The vast majority (96%) of GABAergic synaptic input to SPN somata and proximal dendrites may also be capable of releasing a second inhibitory neurotransmitter, glycine, or 2) the localization of postsynaptic gephyrin does not exclusively identify synaptic sites associated with the presynaptic release of the neurotransmitter glycine.

The first conclusion is not in substantial agreement with existing physiological, pharmacological and anatomical data: 1) Clendening and Hume (1990a,b) have shown in a cell culture system that SPN neurons express receptors for GABA that are distinct from receptors for glycine. Recordings from whole-cell patch-clamped SPNs showed that bath application of GABA resulted in an inward current; the major current-carrying ion was Cl^-; furthermore, responses to GABA were abolished with bath application of the specific $GABA_A$ receptor antagonist bicuculline. 2) Inokuchi et al. (1992) have shown in an in vitro slice preparation that focal stimulation of the lateral funiculus close to the intermediolateral cell column (IML) elicited monosynaptic (presumptively) fast IPSPs within SPNs; one of the populations of fast IPSPs was selectively attenuated or abolished by prior bath application of the $GABA_A$ receptor antagonist bicuculline. 3) Prior light and electron microscopic investigations that focused separately on the identification of $GABA^+$ and $glycine^+$ (more accurately, GABA-like and glycine-like) inputs to the SPNs suggest that it is unlikely that all $GABA^+$ terminals are also $glycine^+$ (Bogan et al., 1989; Cabot et al., 1992). Altogether, these anatomical, physiological, and pharmacological data

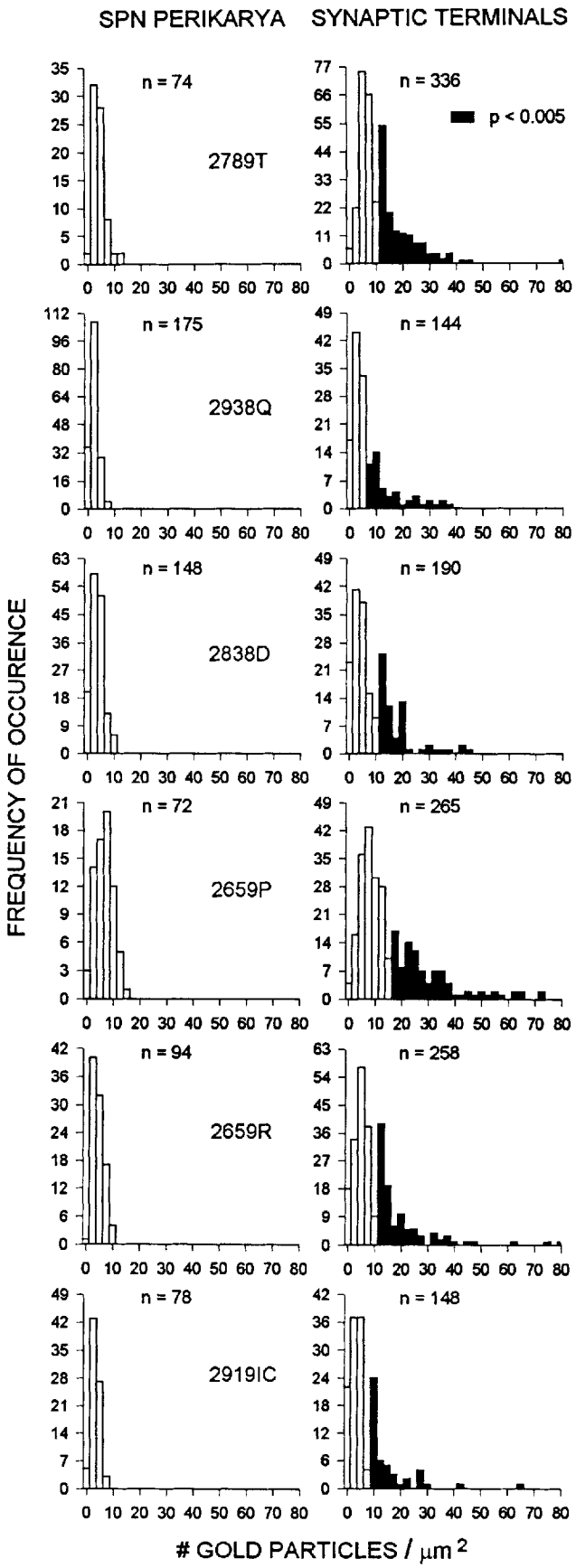

Fig. 5. Histograms of the frequency distributions of GABA-like immunogold labeling in sympathetic preganglionic somata (SPN perikarya) and in synaptic terminals in the SPN neuropil (synaptic terminals). Six separate and independent samples were acquired (see Materials and Methods). Criterion cutoff values for the identification of terminals with significantly elevated levels of GABA-like immunoreactivity (i.e., $GABA^+$ terminals) are listed in Table 1. The darkened portions of the synaptic terminals frequency histograms identify the distributions of $GABA^+$ terminals within the individual samples. n under SPN perikarya: total No. of terminal sample area (TSA) samples. n under Synaptic terminals: No. of synaptic terminals sampled.

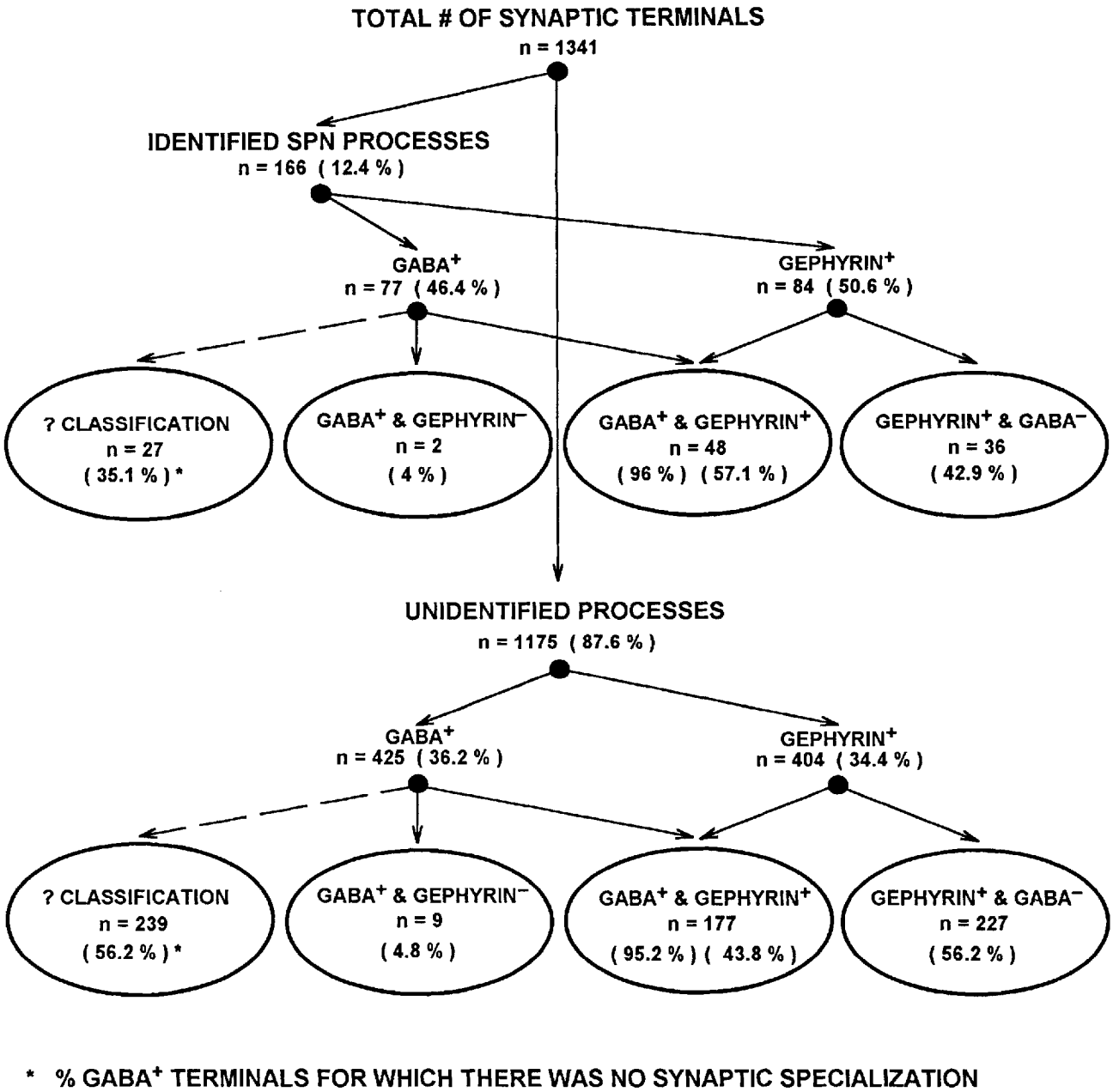

Fig. 6. Schematic flow diagram showing the quantitative relationships between GABA-like immunogold labeling of synaptic terminals ($GABA^+$ and $GABA^-$) and the presence or absence of postsynaptic gephyrin immunostaining ($gephyrin^+$ and $gephyrin^-$). See text for further details.

support the hypothesis that there is an important GABAergic input to SPNs independent of a glycinergic innervation.

If the hypothesis outlined above has merit, then one has to postulate that the nearly one-to-one $GABA^+/gephyrin^+$ relationship observed in the present experiments reflects the likelihood that the presence of postsynaptic gephyrin is not a necessary and sufficient condition to predict presynaptic localization of glycine neurotransmitter. Recent molecular, biochemical, and anatomical investigations strongly support this proposal. First, it has been shown that there are at least five alternatively spliced variants of gephyrin mRNAs present in rat brain (Prior et al., 1992). Second, gephyrin transcripts and gephyrin immunoreactivity are present throughout the mammalian CNS, including regions (e.g., cortex and thalamus) known to lack both a major glycinergic innervation and neuronal expression of mRNA transcripts signaling the subsequent synthesis of the ligand-binding α subunits of the glycine receptor (Kirsch and Betz, 1993; Kirsch et al., 1993a). Third, the distribution of gephryin transcripts most closely parallels the distribution of the nonligand-binding β subunit of the glycine receptor complex (Malosio et al., 1991a; Kirsch et

al., 1993a). These data, in toto, have led to the proposal that gephyrin immunoreactivity is not limited to postsynaptic sites associated with the ligand-binding α subunits of the glycine receptor complex. Indeed, one specific suggestion that has been put forward is that gephyrin may be associated with the $GABA_A$ receptor (Malosio et al., 1991a; Prior et al., 1992; Kirsch and Betz, 1993; Kirsch et al., 1993a). Given the above-mentioned observations and the fact that the monoclonal antibody used in the present experiments (mAb7a) recognizes all known forms gephyrin in the CNS (Kirsch and Betz, 1993), our anatomical data are consistent with the following hypotheses: 1) Postsynaptic gephyrin in SPNs is associated with $GABA_A$ receptors and 2) $GABA^+$ synaptic terminals contacting SPNs, by virtue of their association with postsynaptic gephyrin, do not necessarily contain a second inhibitory amino acid neurotransmitter, glycine.

It is important to recognize that these hypotheses do not exclude the possibility that some fraction of $GABA^+$/$gephyrin^+$ associations predicts colocalization of glycine and GABA neurotransmitters within the same presynaptic afferent terminal. The physiological observations of Inokuchi et al. (1992) provide the strongest data in support of this possibility; they showed that ~20% of fast IPSPs recorded in SPNs following focal stimulation of the lateral funiculus were abolished only by application of both bicuculline and strychnine. Although these data are entirely consistent with the suggestion that GABA and glycine are being coreleased from single boutons, it is also worth pointing out that the anatomical data in this report suggest an alternative interpretation. It was not unusual to observe a close spatial arrangement of $GABA^+$/$gephyrin^+$ and $GABA^-$/$gephryin^+$ associations (see, e.g., Figs. 1, 7). Because focal stimulation of axons was used in the experiments of Inokuchi et al. (1992), it is possible that separate inputs were being coactivated. It is equally plausible that the intracellular recording methods were not sensitive enough to isolate potentially minor differences in the temporal time courses of separate fast IPSPs being generated by simultaneous release of GABA and glycine neurotransmitter from different terminals that have little spatial separation.

In summary, postsynaptic gephyrin immunoreactivity in SPN processes was associated with at least two classes of synaptic inputs to SPNs. One class of terminal input was non-GABAergic (i.e., $GABA^-$); we suggest that many, perhaps all, of these terminals contain glycine neurotransmitter. $GABA^-$/$gephyrin^+$ associations were an anticipated result and were predictable on the basis of prior anatomical, physiological, and pharmacological data. The second class of terminal input associated with postsynaptic gephyrin was GABAergic (i.e., $GABA^+$). The nearly one-to-one correspondence between postsynaptic gephyrin and $GABA^+$ boutons was unexpected. Prior physiological and pharmacological experiments suggest that the hyperpolarizing membrane potentials observed in SPNs following either presynaptic release or exogenous application of GABA are generated by activation of postsynaptic $GABA_A$ receptors. This has led us

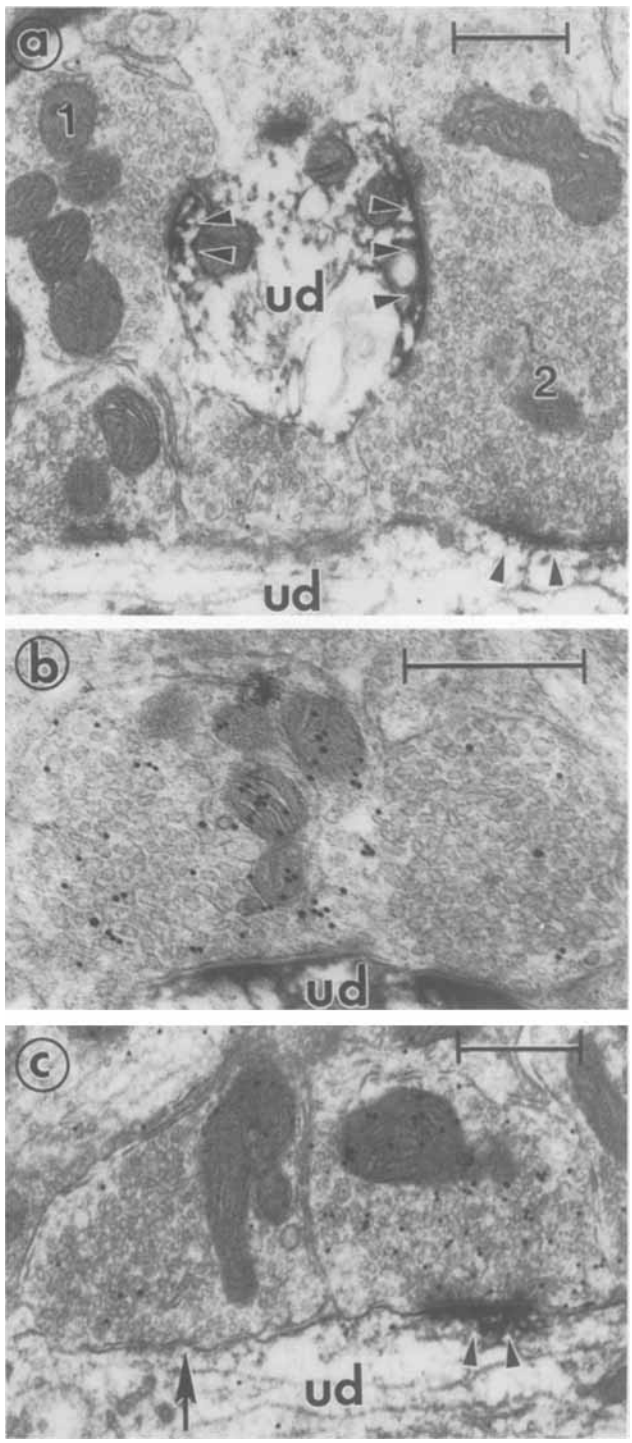

Fig. 7. Electron micrographs showing $GABA^-$/$gephyrin^+$, $GABA^+$/$gephyrin^+$, and $GABA^-$/$gephyrin^-$ associations in the IML neuropil. **a:** Electron micrograph showing postsynaptic gephyrin immunoreactivity (arrowheads) associated with unidentified, small-caliber dendrites (ud) in the IML neuropil. Both synaptic terminals (1, 2) associated with postsynaptic gephyrin in this electron micrograph are $GABA^-$. Synaptic terminal 2 is associated with postsynaptic gephyrin localized to peripheral membrane regions in two different dendrites. **b:** Electron micrograph showing postsynaptic gephyrin immunoreactivity in an unidentified dendrite (ud) receiving synaptic input from two separate boutons. The bouton on the left is immunopositive for GABA (i.e., $GABA^+$); the bouton on the right is $GABA^-$. **c:** Electron micrograph showing an example of $GABA^-$ (terminal on the left) and $GABA^+$ (terminal on the right) synaptic input to an unidentified dendrite (ud) in the IML neuropil. The $GABA^+$ terminal is associated with postsynaptic gephyrin immunoreactivity (arrowheads). The $GABA^-$ terminal is not associated with postsynaptic gephyrin (arrow). Scale bars = 0.5 μm.

to conclude that postsynaptic gephyrin is associated with, and perhaps is involved in the anchoring of, $GABA_A$ receptors in the membranes of SPNs. It has been argued that $GABA^+$/gephyrin$^+$ associations do not, with sufficiency or of necessity, predict colocalization of the two inhibitory amino acid neurotransmitters GABA and glycine within single boutons synapsing on SPN processes.

ACKNOWLEDGMENTS

The authors thank Ms. Wendy Finnegan for her valuable photographic assistance. J.B.C. is supported in part by a MERIT award from the National Heart, Lung, and Blood Institute (HL24103).

LITERATURE CITED

Akagi, H., K. Hirai, and F. Hishinuma (1991a) Cloning of a glycine receptor subtype expressed in rat brain and spinal cord during a specific period of neuronal development. FEBS Lett. *281:*160–166.

Akagi, H., K. Hirai, and F. Hishinuma (1991b) Functional properties of strychnine-sensitive glycine receptors expressed in *Xenopus* oocytes injected with a single mRNA. Neurosci. Res. *11:*28–40.

Altschuler, R.A., H. Betz, M.H. Parakkal, K.A. Reeks, and R.J. Wenthold (1986) Identification of glycinergic synapses in the cochlear nucleus through immunocytochemical localization of the postsynaptic receptor. Brain Res. *369:*316–320.

Backman, S.B., and J.L. Henry (1983) Effects of GABA and glycine on sympathetic preganglionic neurons in the upper thoracic intermediolateral nucleus of the cat. Brain Res. *277:*365–369.

Bacon, S.J., and A.D. Smith (1988) Preganglionic sympathetic neurones innervating the rat adrenal medulla: Immunocytochemical evidence of synaptic input from nerve terminals containing substance P, GABA, or 5-hydroxytryptamine. J. Auton. Nerv. Syst. *24:*97–122.

Becker, C.M., W. Hoch, and H. Betz (1988) Glycine receptor heterogeneity in rat spinal cord during postnatal development. EMBO J. *7:*3717–3726.

Becker, C.M., W. Hoch, and H. Betz (1989) Sensitive immunoassay shows selective association of peripheral and integral membrane proteins of the inhibitory glycine receptor complex. J. Neurochem. *53:*124–131.

Betz, H. (1992) Structure and function of inhibitory glycine receptors. Q. Rev. Biophys. *25:*381–394.

Bogan, N., A. Mennone, and J.B. Cabot (1989) Light microscopic and ultrastructural localization of GABA-like immunoreactive input to retrogradely labeled sympathetic preganglionic neurons. Brain Res. *505:*257–270.

Bormann, J., N. Rundstrom, H. Betz, and D. Langosch (1993) Residues within transmembrane segment M2 determine chloride conductance of glycine receptor homo- and hetero-oligomers. EMBO J. *12:*3729–3737.

Cabot, J.B., V. Alessi, and A. Bushnell (1992) Glycine-like immunoreactive input to sympathetic preganglionic neurons. Brain Res. *571:*1–18.

Cabot, J.B., A. Bushnell, and V. Alessi (1993) Electron microscopic localization of postsynaptic glycine receptor (93 kD) in sympathetic preganglionic neurons: Relationships to GABA and non-GABA synaptic terminals. Soc. Neurosci. Abstr. *19:*1484.

Cabot, J.B., V. Alessi, and A. Bushnell (1994) A quantitative ultrastructural immunogold labeling study of the relationships between glutamate (GLU) and GABA containing boutons synapsing on sympathetic preganglionic neurons. Soc. Neurosci. Abstr. *20:*843.

Chen, S., and D.E. Hillman (1993) Colocalization of neurotransmitters in the deep cerebellar nuclei. J. Neurocytol. *22:*81–91.

Chiba, T., and R. Semba (1991) Immuno-electronmicroscopic studies on the gamma-aminobutyric acid and glycine receptor in the intermediolateral nucleus of the thoracic spinal cord of rats and guinea pigs. J. Auton. Nerv. Syst. *36:*173–182.

Clendening, B., and R.I. Hume (1990a) Expression of multiple neurotransmitter receptors by sympathetic preganglionic neurons in vitro. J. Neurosci. *10:*3977–3991.

Clendening, B., and R.I. Hume (1990b) Cell interactions regulate dendritic morphology and responses to neurotransmitters in embryonic chick sympathetic preganglionic neurons in vitro. J. Neurosci. *10:*3992–4005.

Dun, N.J., and N. Mo (1989) Inhibitory postsynaptic potentials in neonatal rat sympathetic preganglionic neurones in vitro. J. Physiol. (London) *410:*267–281.

Froehner, S.C. (1993) Anchoring glycine receptors. Nature *366:*719.

Graham, D., F. Pfeiffer, and H. Betz (1985) Purification and characterization of the glycine receptor of pig spinal cord. Biochemistry *24:*990–994.

Grenningloh, G., V. Schmieden, P.R. Schofield, P.H. Seeburg, T. Siddique, T.K. Mohandas, C.-M. Becker, and H. Betz (1990) Alpha subunit variants of the human glycine receptor: Primary structures, functional expression and chromosomal localization of the corresponding genes. EMBO J. *9:*771–776.

Grünert, U., and H. Wässle (1993) Immunocytochemical localization of glycine receptors in the mammalian retina. J. Comp. Neurol. *335:*523–537.

Hoch, W., H. Betz, and C.-M. Becker (1989) Primary cultures of mouse spinal cord express the neonatal isoform of the inhibitory glycine receptor. Neuron *3:*339–348.

Inokuchi, H., M. Yoshimura, A. Trzebski, C. Polosa, and S. Nishi (1992) Fast inhibitory postsynaptic potentials and responses to inhibitory amino acids of sympathetic preganglionic neurons in the adult cat. J. Auton. Nerv. Syst. *41:*53–60.

Kirsch, J., and H. Betz (1993) Widespread expression of gephyrin, a putative glycine receptor-tubulin linker protein, in rat brain. Brain Res. *621:*301–310.

Kirsch, J., D. Langosch, P. Prior, B. Schmitt, and H. Betz (1991) The 93-kDa glycine receptor-associated protein binds tubulin. J. Biol. Chem. *266:*22242–22245.

Kirsch, J., M.L. Malosio, I. Wolters, and H. Betz (1993a) Distribution of gephyrin transcripts in the adult and developing rat brain. Eur. J. Neurosci. *5:*1109–1117.

Kirsch, J., I. Wolters, A. Triller, and H. Betz (1993b) Gephyrin antisense oligonucleotides prevent glycine receptor clustering in spinal neurons. Nature *366:*745–748.

Kuhse, J., V. Schmieden, and H. Betz (1990a) A single amino acid exchange alters the pharmacology of neonatal rat glycine receptor subunit. Neuron *5:*867–873.

Kuhse, J., V. Schmieden, and H. Betz (1990b) Identification and functional expression of a novel ligand binding subunit of the inhibitory glycine receptor. J. Biol. Chem. *265:*22317–22320.

Kuhse, J., B. Laube, D. Magalei, and H. Betz (1993) Assembly of the inhibitory glycine receptor: Identification of amino acid sequence motifs governing subunit stoichiometry. Neuron *11:*1049–1056.

Langosch, D., C.-M. Becker, and H. Betz (1990) The inhibitory glycine receptor: A ligand-gated chloride channel of the central nervous system. Eur. J. Biochem. *194:*1–8.

Llewellyn-Smith, I.J., K.D. Phend, J.B. Minson, P.M. Pilowsky, and J.P. Chalmers (1992) Glutamate-immunoreactive synapses on retrogradely-labelled sympathetic preganglionic neurons in rat spinal cord. Brain Res. *581:*67–80.

Malosio, M.-L., B. Marquez-Poucy, J. Kuhse, and H. Betz (1991a) Widespread expression of glycine receptor subunit mRNAs in the adult and developing brain. EMBO J. *10:*2401–2409.

Malosio, M.-L., G. Grenningloh, J. Kuhse, V. Schmieden, B. Schmitt, P. Prior, and H. Betz (1991b) Alternative splicing generates two variants of the α subunit of the inhibitory glycine receptor. J. Biol. Chem. *266:*2048–2053.

Mitchell, K., R.C. Spike, and A.J. Todd (1993) An immunocytochemical study of glycine receptor and GABA in laminae I–III of rat spinal dorsal horn. Neuroscience *13:*2371–2381.

Mo, N., and N.J. Dun (1987) Is glycine an inhibitory transmitter in rat lateral horn cells? Brain Res. *400:*139–144.

Nicola, M.A., C.-M. Becker, and A. Triller (1992) Development of glycine receptor alpha subunit in cultivated rat spinal neurons: An immunocytochemical study. Neurosci. Lett. *138:*173–178.

Pfeiffer, F., D. Graham, and H. Betz (1982) Purification by affinity chromatography of the glycine receptor of rat spinal cord. J. Biol. Chem. *257:*9389–9393.

Pfeiffer, F., R. Simler, G. Grenningloh, and H. Betz (1984) Monoclonal antibodies and peptide mapping reveal structural similarities between the subunits of the glycine receptor of rat spinal cord. Proc. Natl. Acad. Sci. USA *81:*7224–7227.

Pourcho, R.G., and M.T. Owczarzak (1991) Connectivity of glycine immunoreactive amacrine cells in the cat retina. J. Comp. Neurol. *307:*549–561.

Prior, P., B. Schmitt, G. Grenningloh, I. Pribilla, G. Multhaup, K. Beyreuther, Y. Maulet, P. Werner, D. Langosch, J. Kirsch, and H. Betz (1992) Primary structure and alternative spice variants of gephyrin, a putative glycine receptor-tubulin linker protein. Neuron *8:*1161–1170.

Sassoè-Pognetto, M., H. Wässle, and U. Grünert (1994) Glycinergic synapses

in the rod pathway of the rat retina: Cone bipolar cells express the α1 subunit of the glycine receptor. J. Neurosci. *14:*5131–5146.

Schmieden, V., G. Grenningloh, P.R. Schofield, and H. Betz (1989) Functional expression in *Xenopus* oocytes of the strychnine binding 48 kd subunit of the glycine receptor. EMBO J. *8:*695–700.

Schmieden, V., J. Kuhse, and H. Betz (1992) Agonist pharmacology of neonatal and adult glycine receptor alpha subunits: Identification of amino acid residues involved in taurine activation. EMBO J. *11:*2025–2032.

Schmitt, B., P. Knaus, C.M. Becker, and H. Betz (1987) The Mr 93000 polypeptide of the postsynaptic glycine receptor is a peripheral membrane protein. Biochemistry *26:*805–811.

Seitanidou, T., A. Triller, and H. Korn (1988) Distribution of glycine receptors on the membrane of a central neuron: An immunoelectron microscopy study. J. Neurosci. *8:*4319–4333.

Smiley, J.F., and S. Yazulla (1990) Glycinergic contacts in the outer plexiform layer of the *Xenopus laevis* retina characterized by antibodies to glycine, GABA, and glycine receptor. J. Comp. Neurol. *299:*375–388.

Snedecor, G.W., and W.G. Cochran (1989) Statistical Methods. Ames, IA: Iowa State University Press.

Somogyi, P., and I. Soltesz (1986) Immunogold demonstration of GABA in synaptic terminals of intracellularly recorded, horseradish peroxidase-filled basket cells and clutch cells in the cat's visual cortex. Neuroscience *19:*1051–1065.

Triller, A., F. Cluzeaud, F. Pfieffer, H. Betz, and H. Korn (1985) Distribution of glycine receptors at central synapses: An immunoelectron microscopy study. J. Cell Biol. *101:*683–688.

Triller, A., F. Cluzeaud, and H. Korn (1987) Gamma aminobutyric acid-containing terminals can be apposed to glycine receptors at central synapses. J. Cell Biol. *104:*947–956.

van den Pol, A.N., and T. Gorcs (1988) Glycine and glycine receptor immunoreactivity in brain and spinal cord. J. Neurosci. *8:*472–492.

Vandenberg, R.J., C.R. French, P.H. Barry, J. Shine, and P.R. Schofield (1992a) Antagonism of ligand-gated ion channel receptors: Two domains of the glycine receptor alpha subunit form the strychnine-binding site. Proc. Natl. Acad. Sci. USA *89:*1765–1769.

Vandenberg, R.J., C.A. Handford, and P.R. Schofield (1992b) Distinct agonist- and antagonist-binding sites on the glycine receptor. Neuron *9:*491–496.

Wenthold, R.J., M.H. Parakkal, M.D. Oberdorfer, and R.A. Altschuler (1988) Glycine receptor immunoreactivity in the ventral cochlear nucleus of the guinea pig. J. Comp. Neurol. *276:*423–435.

Yazulla, S., and K.M. Studholme (1991) Glycine-receptor immunoreactivity in retinal bipolar cells is postsynaptic to glycinergic and GABAergic amacrine cell synapses. J. Comp. Neurol. *310:*11–20.

Zucker, C.L., and B. Ehinger (1992) Heterogeneity of receptor immunoreactivity at synapses of glycine-utilizing neurons. Proc. R. Soc. London [Biol.] *249:*89–94.